



Feasibility of low-dose CT with model-based iterative image reconstruction in follow-up of patients with testicular cancer



Kevin P. Murphy^{a,b,c}, Lee Crush^{b,c}, Siobhan B. O'Neill^{a,c}, James Foody^d, Micheál Breen^e, Adrian Brady^c, Paul J. Kelly^f, Derek G. Power^g, Paul Sweeney^h, Jackie Byeⁱ, Owen J. O'Connor^{a,b,c}, Michael M. Maher^{a,b,c}, Kevin N. O'Regan^{a,*}

^a Department of Radiology, Cork University Hospital, Cork, Ireland

^b Department of Radiology, University College Cork, Cork, Ireland

^c Department of Radiology, Mercy University Hospital, Cork, Ireland

^d Department of Electrical and Electronic Engineering, University College Cork, Cork, Ireland

^e Department of Radiology, Boston Children's Hospital, 300 Longwood Avenue, Boston, MA 02115, USA

^f Department of Radiation Oncology, Cork University Hospital, Cork, Ireland

^g Department of Medical Oncology, Cork and Mercy University Hospitals, Cork, Ireland

^h Department of Urology, Mercy University Hospital, Cork, Ireland

ⁱ General Electric Healthcare Technologies, Herdfordshire, UK

ARTICLE INFO

Article history:

Received 28 October 2015

Received in revised form 18 January 2016

Accepted 20 January 2016

Available online 16 February 2016

Keywords:

Testicular cancer

Radiation dose

Low-dose computed tomography

Iterative reconstruction

Model-based iterative reconstruction

ABSTRACT

Purpose: We examine the performance of pure model-based iterative reconstruction with reduced-dose CT in follow-up of patients with early-stage testicular cancer.

Methods: Sixteen patients (mean age 35.6 ± 7.4 years) with stage I or II testicular cancer underwent conventional dose (CD) and low-dose (LD) CT acquisition during CT surveillance. LD data was reconstructed with model-based iterative reconstruction (LD-MBIR). Datasets were objectively and subjectively analysed at 8 anatomical levels. Two blinded clinical reads were compared to gold-standard assessment for diagnostic accuracy.

Results: Mean radiation dose reduction of 67.1% was recorded. Mean dose measurements for LD-MBIR were: thorax – 66 ± 11 mGy cm (DLP), 1.0 ± 0.2 mSv (ED), 2.0 ± 0.4 mGy (SSDE); abdominopelvic – 128 ± 38 mGy cm (DLP), 1.9 ± 0.6 mSv (ED), 3.0 ± 0.6 mGy (SSDE). Objective noise and signal-to-noise ratio values were comparable between the CD and LD-MBIR images. LD-MBIR images were superior ($p < 0.001$) with regard to subjective noise, streak artefact, 2-plane contrast resolution, 2-plane spatial resolution and diagnostic acceptability. All patients were correctly categorised as positive, indeterminate or negative for metastatic disease by 2 readers on LD-MBIR and CD datasets.

Conclusions: MBIR facilitated a 67% reduction in radiation dose whilst producing images that were comparable or superior to conventional dose studies without loss of diagnostic utility.

© 2016 The Authors. Published by Elsevier Ltd. This is an open access article under the CC BY-NC-ND license (<http://creativecommons.org/licenses/by-nc-nd/4.0/>).

1. Introduction

Ionising radiation from medical imaging accounts for significantly increasing radiation exposure amongst the general

population worldwide [1]. The majority of medical imaging radiation comes from computed tomography (CT) procedures, and patients who undergo frequent CT examinations may be at increased risk of radiation-induced malignancies [2]. Radiation dose-reduction strategies are the subject of ongoing studies.

Testis germ cell tumour (GCTs) are a curable cancer in the majority of patients [3]. The most common site of metastatic spread is retroperitoneal lymph nodes and CT is the most commonly used imaging modality for surveillance of patients with early stage disease after orchidectomy. CT surveillance is standard of care and critical in identifying recurrent disease, such that it can be treated with curative intent. Surveillance recommendations vary as to the

* Corresponding author. Fax: +353 21 4920319.

E-mail addresses: thekpm@gmail.com (K.P. Murphy), lcrush@muh.ie (L. Crush), siobhanxx@gmail.com (S.B. O'Neill), james@ayda.co (J. Foody), Micheal.Breen@childrens.harvard.edu (M. Breen), abrady@muh.ie (A. Brady), PaulJ.Kelly@hse.ie (P.J. Kelly), dpower@muh.ie (D.G. Power), psweeney@muh.ie (P. Sweeney), jackie.bye@ge.com (J. Bye), ojoconnor@ucc.ie (O.J. O'Connor), m.maher@ucc.ie (M.M. Maher), Kevin.ORegan1@hse.ie (K.N. O'Regan).

number of CT examinations required, and length of follow-up but the majority of patients require multiple abdominopelvic CTs over the course of 5–10 follow-up years [4,5].

There is emerging data that patients with stage I seminoma are at increased risk of second malignancy, in addition to cardiovascular complications, as a result of adjuvant radiation therapy [6–9]. In theory, the additional radiation dose from serial CTs could increase these risks further, particularly in younger patients. Radiation dose from CT surveillance of testicular cancer patients is not insignificant with median lifetime cumulative effective doses (CED) from 125 mSv [10] to in excess of 200 mSv [11]. These values are in excess of median doses received by patient groups with non-neoplastic chronic diseases that are considered at risk for high lifetime CED [12–15].

Iterative reconstruction is a CT image reconstruction method that results in decreased image noise and increased spatial resolution. Hybrid iterative reconstruction with low-dose CT has undergone considerable research [16–18] and is now being widely used. The use of pure, model-based iterative reconstruction (MBIR) in CT has been recently investigated [19–22] enabling dose reductions in excess of 65%.

No study has specifically examined the use of pure iterative reconstruction as a dose reduction technique in follow-up of testicular cancer patients. With this in mind, we designed a prospective study to evaluate the performance of MBIR in low-dose CT assessment of patients undergoing surveillance for stage I or II testicular cancer.

2. Materials and methods

Following ethical approval from the institutional clinical ethics research committee, a prospective HIPAA compliant study design was utilised. The study was limited to patients with stage I or II testicular GCT, undergoing surveillance imaging of a previously diagnosed and staged testicular cancer. The staging used was per American Joint Committee on Cancer (AJCC) TNM Staging Systemic for Testis Cancer (7th ed., 2010). Patients were recruited from medical oncology and radiation oncology services at two tertiary referral centres during outpatient clinic visits. Following a detailed discussion, each patient signed an ethics board approved consent form. Exclusion criteria included age <18 years, no previous staging studies, unknown/equivocal histology, \geq stage III disease and patient refusal.

All patients were scanned using a 128-slice multidetector CT scanner (General Electric Discovery 750HD, GE Medical Systems, Milwaukee, WI) using oral and intravenous contrast material. A standardised 100 ml intravenous contrast bolus (Iohexol, Omnipaque 300, GE Healthcare, Mississauga, ON) was delivered at 2.5 ml/s. The referring clinician determined whether CT thorax–abdomen–pelvis or CT abdomen–pelvis were to be performed. Two contemporaneous CT scans were acquired, with a 6 s delay, both imaging identical anatomic areas. The low-dose protocol (LD) was designed in conjunction with the manufacturers using phantom data to impart a radiation dose of 20–30% of a routine departmental CT. The second, conventional dose (CD) protocol was designed to impart an ED (effective dose) of 70–80% of a routine CT scan. Thus, patient study participation did not result in increased radiation dose. LD CT thorax/abdomen–pelvis employed tube voltages of 100 kV/120 kV, rotation times 0.5 s/0.8 s, z-axis automated tube–current modulation (ATCM) with minimum and maximum current thresholds of 20 and 130 mA/60 and 160 mA, respectively, and noise indices of 70/41.99. CD CT thorax/abdomen–pelvis employed tube voltages of 100 kV/120 kV, rotation times 0.8 s/0.8 s, z-axis ATCM with current thresholds of 50 and 200 mA/120 and 200 mA, respectively, and noise indices of 34/35.36. Images were

acquired at 0.625 mm and reconstructed to 2 mm slices. LD CT data were reconstructed using a pure iterative reconstruction algorithm (model-based iterative reconstruction, MBIR, Veo, GE Healthcare, GE Medical Systems, Milwaukee, WI) (LD–MBIR). CD CT images were reconstructed with 60% FBP (filtered back projection) and 40% ASiR (adaptive statistical iterative reconstruction, GE Healthcare) (CD–ASiR) consistent with manufacturer recommendations and standard departmental CT reconstruction protocol.

2.1. Quantitative analysis of image noise and SNR

LD–MBIR and CD–ASiR images were objectively and subjectively assessed for image quality. Objective noise was assessed by a single reader (KM, 7 years experience). Spherical regions of interest (ROIs) (diameter, 10 mm; volume, 519 mm³) were placed in the following 8 anatomic locations: right supraspinatus muscle at level of glenoid (level 1), erector spinae at level of carina (level 2), liver at diaphragm (level 3), liver at porta hepatis (level 4), right renal cortex at renal hilum (level 5), erector spinae at level of right kidney lower pole (level 6), psoas muscle at iliac crest (level 7) and gluteus maximus at level of the acetabular roof (level 8). These measurements were performed using a commercial workstation (Advantage Workstation VolumeShare 2, Ver4.4, GE Medical Systems, Milwaukee, WI). At each level, efforts were made to place the ROI in as homogenous an area as possible, away from blood vessels etc. Each reconstruction pertaining to a given patient was simultaneously loaded on the workstation and an ROI was placed on a dataset, which automatically generated ROIs on the matched images on the other reconstructions. Mean HU attenuation and HU ROI standard deviation (SD) were recorded for all datasets. The latter of these served as an objective measure of noise with signal-to-noise ratio (SNR) being calculated by dividing mean HU by HU SD.

Objective noise was further assessed via a second automated measurement technique that comprised three steps: edge detection was performed to detect contours, an iterative algorithm located homogenous 10 mm ROIs by discounting ROIs which encompassed any edges/contours highlighted by step one and SDs of all homogenous ROIs were computed with the lowest four values being averaged to yield an objective noise measurement. This technique was implemented using Matlab® programming language.

2.2. Subjective image quality

Subjective image quality was assessed by 2 readers in consensus (KM, MM [20 years experience]), using previously validated methods at the eight levels. Diagnostic acceptability, subjective image noise and spatial resolution and were scored using a ten-point scale, and streak artefact was scored on a three-point scale. Diagnostic acceptability was graded as acceptable (score of 5), unacceptable (score of 1) or excellent (score of 10) respectively, according to depiction of soft-tissue structures for diagnostic interpretation and degree of image degradation by artefacts. Subjective image noise was graded according to the extent of “graininess”/“mottle” present on CT images and was graded as acceptable (score of 5) if average graininess with satisfactory depiction of small anatomic structures (e.g. blood vessels) and tissue interfaces was seen, unacceptable (score of 1) if graininess interfered with structure depiction, and excellent (score of 10) if there was minimal/no mottle. Regarding contrast resolution, a score of 10 represented superior contrast depiction between different soft tissues, a score of 1 indicated poorest contrast and 5 indicated acceptable contrast. The presence and impact of streak artefact was scored at each anatomical level using a 3-point scheme (0 - no streak artefact; 1 - streak artefact present

but not interfering with interpretation; 2 - streak artefact present and interfering with interpretation).

2.3. Diagnostic accuracy

The presence of findings on LD-MBIR and CD-ASiR images was likewise evaluated independently in a blinded fashion by two fellowship-trained radiology attendings/consultants (AB, KOR) [27 and 9 years radiology experience, respectively]. To minimise effects of recall bias, all datasets were anonymised and reviewed in a random patient order. In addition, a six-week delay was instituted between review of LD-MBIR and CD-ASiR images. Images were reviewed on 2 mm axial and coronal reformats on soft-tissue, bone and lung window settings, using the aforementioned commercial workstation. Readers recorded whether pulmonary nodules, enlarged mediastinal lymph nodes, abdominal visceral lesions, abnormal retroperitoneal lymph nodes or osseous abnormalities were present or absent, in addition to noting the size of the largest lesion at these sites. Readers documented if CT findings were thought to be positive, indeterminate or negative for metastatic disease. Finally, the presence of incidental findings was acknowledged. A similar but un-blinded 'gold-standard' clinical read, where prior studies and all clinical details were available, was performed by 2 radiologists in consensus (KM, MM). Subsequent follow-up imaging was monitored for metastatic disease.

2.4. Radiation dose

Regarding radiation dose parameters, dose length product (DLP) was recorded for each examination. Estimated Dose (ED) (utilising ICRP 103 [23] compliant CT patient dosimetry calculator (ImpACT, London, England)) and size-specific dose estimates (SSDE) (per American Association of Physicists in Medicine (AAPM)) guidelines [24,25] for each study were also calculated.

Patient height, weight and body mass index (BMI) at the time of CT were recorded.

All statistical tests were performed with Statistical Package for Social Sciences (SPSS) version 21.0 (IBM, Armonk, NY). Wilcoxon signed rank test was used for statistical analysis to compare qualitative parameters. Normally distributed quantitative indices were compared using paired *t*-test. A *p*-value of <0.05 was considered statistically significant. All data are presented as mean \pm standard deviation (SD) unless otherwise stated.

3. Results

Sixteen patients with a mean age of 35.6 ± 7.4 years (range 24–47 years) participated. All patients referred for inclusion agreed to participate. Mean BMI was 26.7 ± 3.9 kg/m² (range 20.7–32.9 kg/m²). 11 patients underwent CT thorax–abdomen–pelvis and 5 underwent abdominopelvic CT alone. The following histological subtypes were recorded: seminoma (8 patients), non-seminomatous GCT (5 patients) and mixed type (3 patients). 15 of the patients had stage I disease at diagnosis and 1 patient had stage II disease with prior retroperitoneal lymph node dissection.

3.1. Radiation dose

CD-ASiR thoracic CTs had the following mean radiation dose parameters: 197 ± 52 mGy cm (DLP), 3.2 ± 0.8 mSv (ED), 5.8 ± 1.4 mGy (SSDE). LD-MBIR thoracic studies mean radiation factors were 66 ± 11 mGy cm (DLP), 1.0 ± 0.2 mSv (ED) and 2.0 ± 0.4 mGy (SSDE).

Regarding abdominopelvic CTs, CD-ASiR mean radiation doses were 395 ± 95 mGy cm (DLP), 5.9 ± 1.4 mSv (ED) and

9.3 ± 1.6 mGy (SSDE). Mean LD-MBIR abdominopelvic CT doses were 128 ± 38 mGy cm (DLP), 1.9 ± 0.6 mSv (ED) and 3.0 ± 0.6 mGy (SSDE). A mean dose reduction of $67.1 \pm 4.0\%$ was recorded between LD-MBIR and CD-ASiR studies (using DLP measurements). Using the summated dose of both LD and CD studies that each patient received as a measure of what the patient would receive if not included in this study and had undergone standard departmental protocol, LD-MBIR studies achieved a mean reduction of $75.3 \pm 2.3\%$.

3.2. Quantitative analysis of image noise and SNR

Objective image noise and SNR were evaluated at the 8 levels described above. Fig. 1 demonstrates mean and SD of mean noise measurements for CD-ASiR and LD-MBIR images. There was no significant difference between datasets at any of the 8 levels (*p*-values: 0.132–0.814). When mean objective noise measurements for all levels were compared for datasets, LD-MBIR noise levels (27.55 ± 8.12) were insignificantly lower than CD-ASiR values (27.68 ± 9.01 ; *p* = 0.873).

Results of objective SNR are displayed in Fig. 2. There was no significant difference between CD-ASiR and LD-MBIR images at any of the 8 levels (*p*-values: 0.201–0.897). For all level SNR calculations, LD-MBIR values (3.62 ± 1.99) were insignificantly superior to CD-ASiR calculations (3.53 ± 2.02 ; *p* = 0.510).

Regarding the second objective noise method, despite producing lower SD values than the previous objective assessment, there was again no significant difference between datasets at any of the 8 levels. However, when mean objective noise measurements for all levels were compared for the datasets, LD-MBIR noise levels (23.28 ± 6.77) were insignificantly higher than CD-ASiR values (23.11 ± 7.44 ; *p* = 0.859).

3.3. Subjective image quality

No significant difference was found across 8 anatomical levels for each subjective parameter, hence mean values for all levels were summated to compare LD-MBIR and CD-ASiR quality. LD-MBIR scores were significantly superior (*p* < 0.001 for all comparisons) to CD-ASiR values in terms of subjective noise (9 ± 0 [median \pm interquartile range] vs. 7 ± 0), streak artefact (0 ± 0 vs. 1 ± 0), axial contrast resolution (9 ± 0 vs. 7 ± 1), axial spatial resolution (9 ± 1 vs. 8 ± 0), coronal contrast resolution (9 ± 1 vs. 8 ± 0), coronal spatial resolution (9 ± 1 vs. 8 ± 0), axial diagnostic acceptability (9 ± 1 vs. 8 ± 1) and coronal diagnostic acceptability (9 ± 0 vs. 8 ± 1) (Fig. 3).

3.4. Diagnostic accuracy

Of the 16 patients in the study, none had confirmed metastatic disease on study imaging or on subsequent follow-up (mean follow-up 19.13 ± 5.0 months). Thirteen had no findings, per 'gold-standard' analysis, that were concerning for metastatic recurrence. Three of 16 patients had indeterminate findings for metastatic disease. Of these, 2 patients had retroperitoneal lymph nodes of 10–11 mm in short axis diameter (Figs. 4 and 5) and 1 patient had multiple small non-calcified pulmonary nodules (Fig. 6). Both reader 1 and reader 2 accurately stratified all 16 patients as being indeterminate or negative for metastatic disease, where applicable, on both CD-ASiR and LD-MBIR images, hence showing complete 'gold-standard' correlation.

Reader 1 recorded the same 17 incidental findings on both CD-ASiR and LD-MBIR studies. Reader 2 documented 17 incidental findings on LD-MBIR studies and 15 on CD-ASiR images. These included calcified pulmonary granulomata, aberrant right subclavian artery, hepatic cysts (Figs. 7 and 8), renal scarring, benign

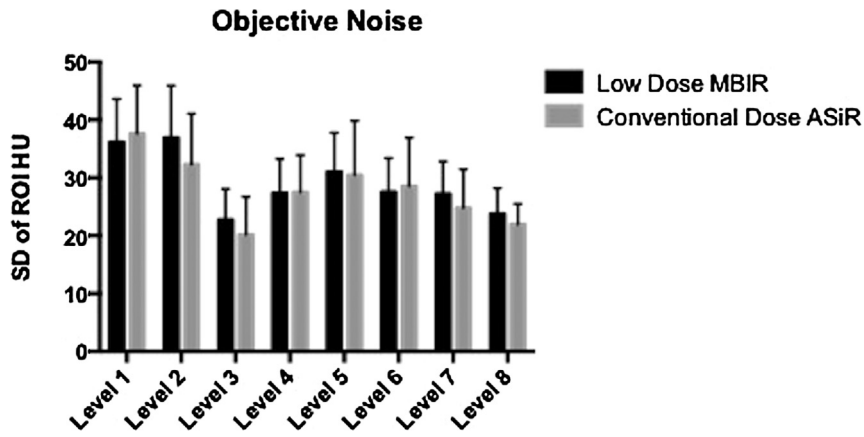


Fig 1. Objective image noise assessment at the 8 assessed levels: right supraspinatus muscle at the level of the glenoid (level 1), erector spinae at the level of the carina (level 2), liver at diaphragm (level 3), liver at porta hepatis (level 4), right renal cortex at the renal hilum (level 5), erector spinae at level of the right kidney lower pole (level 6), psoas muscle at the iliac crest (level 7) and gluteus maximus at the level of the acetabular roof (level 8).

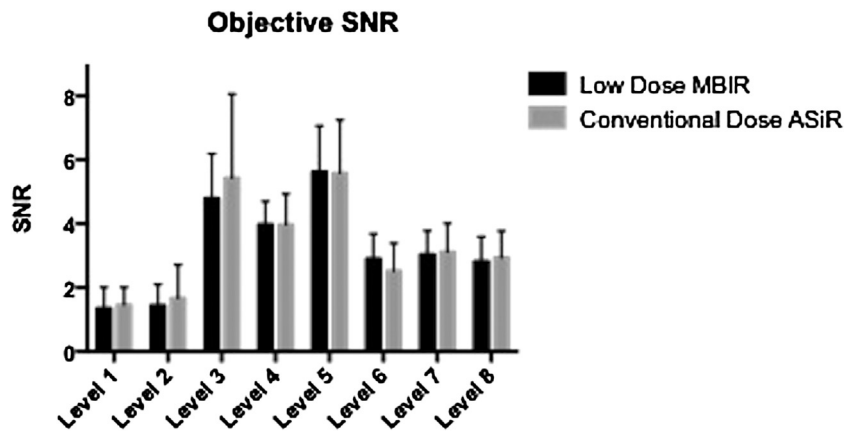


Fig. 2. Objective signal-to-noise ratio (SNR) at the 8 assessed levels.

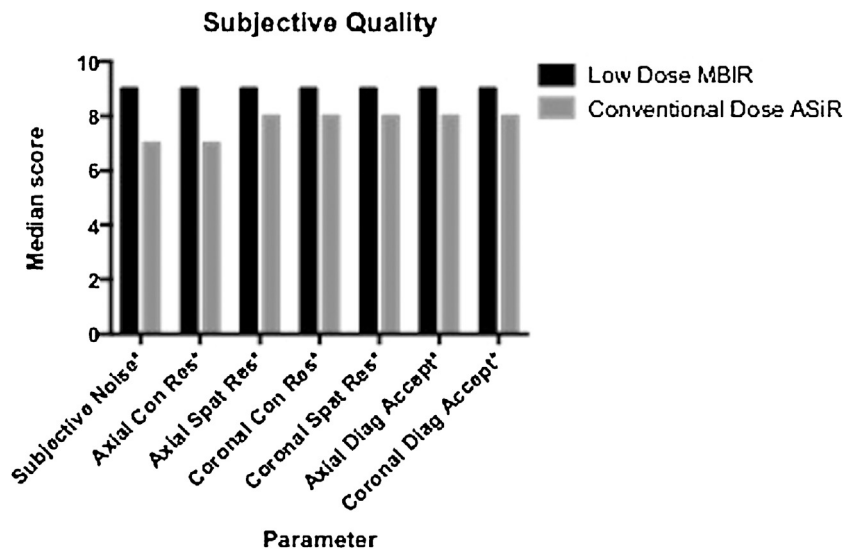


Fig. 3. Subjective image quality analysis. LD-MBIR images were significantly superior ($p < 0.001$) for all recorded factors.

osseous sclerosis/bone islands and degenerative vertebral disease. The 'gold-standard' analysis identified 24 potential incidental findings. Of these, only 2 were deemed as 'likely to be clinically significant' according to ACR RadPeer scoring system [26]. One of these was enlargement of the thymic remnant, which was identified by

both blinded readers on LD-MBIR and CD-ASiR images. The second was a 24 mm lesion abutting the gallbladder that was isodense to adjacent liver, and was identified by reader 2 on the CD-ASiR images. Reader 2 did not identify the lesion on LD-MBIR images and reader 1 did not pinpoint it on either LD-MBIR or CD-ASiR recon-

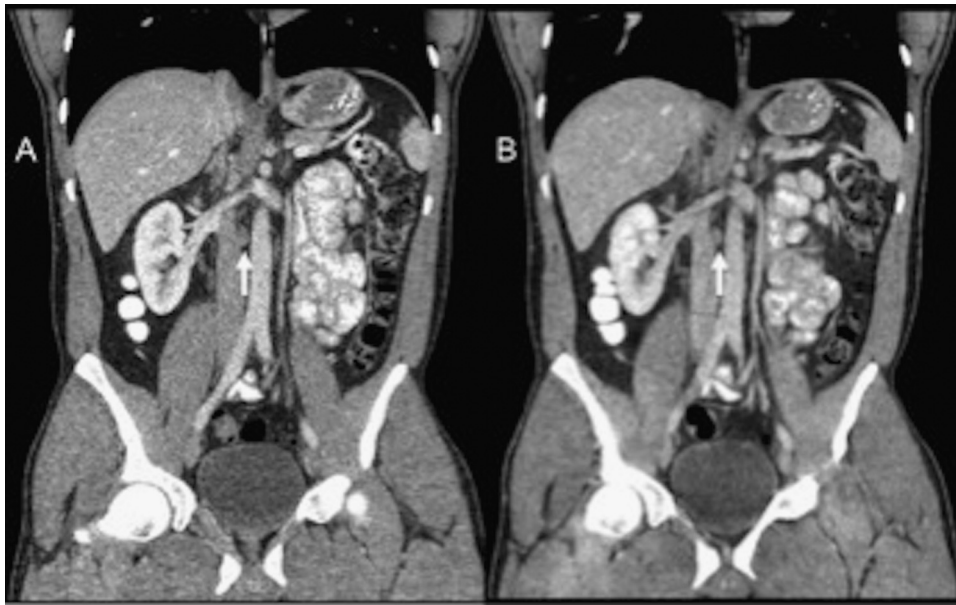


Fig. 4. Coronal CT images of the abdomen in a 36-year-old patient (BMI 20.7 kg/m²) who underwent low-dose CT of the abdomen–pelvis (B) with estimated effective dose of 0.97 mSv (ED). Mildly enlarged retroperitoneal nodes (arrows) are clearly seen on both CD–ASiR (A) and LD–MBIR (B) images.

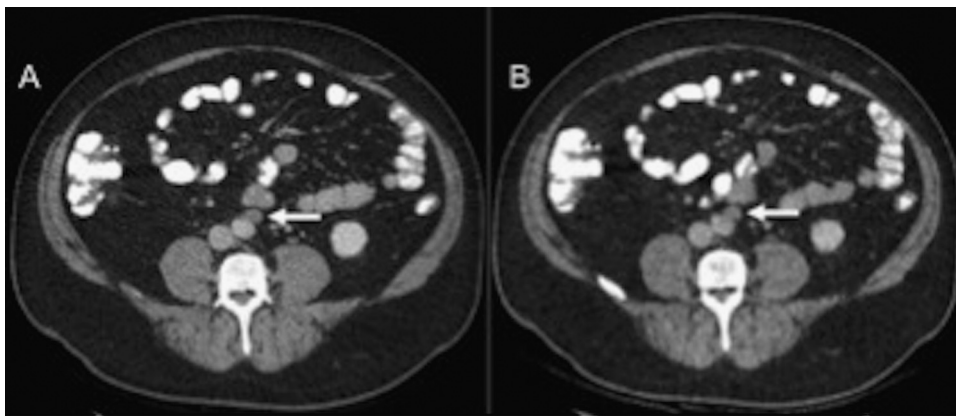


Fig. 5. Axial CT images of the abdomen in a 47-year-old patient (BMI 28.6 kg/m²) with an estimated effective dose (ED) of 3.1 mSv for the low-dose thorax–abdomen–pelvis study (B). A mildly enlarged lymph node anterior to the abdominal aorta (arrows) is evident on both CD–ASiR (A) and LD–MBIR (B) studies.

structions. This abnormality, with the benefit of prior studies and full clinical information, was deemed to be a haematoma from prior surgery and was graded as ‘2b’ (‘discrepancy in interpretation/not ordinarily expected to be made’) per RadPeer [26].

4. Discussion

Patients with testicular cancer, particularly those with stage I–II disease, have an excellent prognosis, tend to be young and are potentially at risk of high lifetime CED, given the intense CT surveillance strategies recommended by international guidelines. Multiple clinical series, of over 1200 patients, with early stage seminoma managed by post-orchidectomy surveillance, have reported recurrence rates of 15–20% and nearly all of these patients are cured with either chemotherapy or radiotherapy. Regular surveillance is therefore critical. Exposure to high doses of ionising radiation can potentially lead to organ dysfunction and malignancy. In a patient group with a curable malignancy, this is especially relevant. Hence, this patient group are an ideal cohort to consider for reduced dose CT scanning as part of clinical surveillance for metastatic disease.

In our study, mean ED of 1.05 ± 0.17 mSv (65.65 ± 10.7 mGy cm (DLP)) and 1.92 ± 0.57 mSv (128.02 ± 38.3 mGy cm (DLP)) for low-

dose thoracic and abdominopelvic CT examinations, respectively, were achieved. These values were obtained at a 67% mean reduction when compared with the CD studies and a 75% average reduction when compared with an estimated standard departmental protocol. Despite this dose reduction, LD–MBIR image quality was comparable to CD–ASiR studies with regard to objective image quality analysis and superior in terms of subjective quality assessment. Blinded image interpretation showed complete agreement in identifying patients with findings negative or indeterminate for metastatic disease when compared with un-blinded gold-standard assessment.

Radiation dose measurements are considerably superior to prior investigations of low-dose testicular cancer CT imaging [27,28]. O’Malley et al. achieved a mean low-dose abdominopelvic CT DLP of 452 mGy cm, which is ~ 3.5 times greater than the mean ED achieved in our study. Gnannt et al. achieved a mean DLP of 636.9 mGy cm for low-dose abdominopelvic CT with ATCM, which is substantially higher than in our study. Prior publications on low-dose CT use in other oncology patient groups, such as lymphoma patients, have achieved dose reductions of approximately 50% [29]. Our current study represents a more substantial dose reduction in a similar patient group.

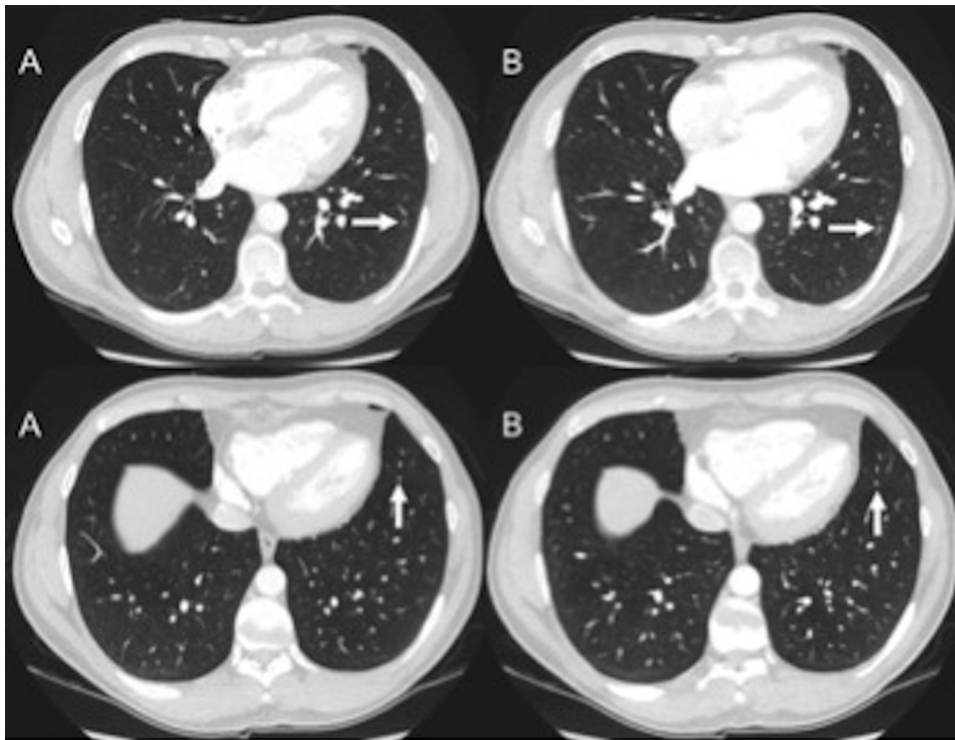


Fig. 6. Axial CT images of the chest in a 36-year-old patient (BMI 21.0 kg/m²) with an estimated effective dose of 1.86 mSv ED for the low-dose thorax–abdomen–pelvis study (B). Subcentimetre pulmonary nodules (arrows) are clearly visible on both CD–ASiR (A) and LD–MBiR (B) datasets.

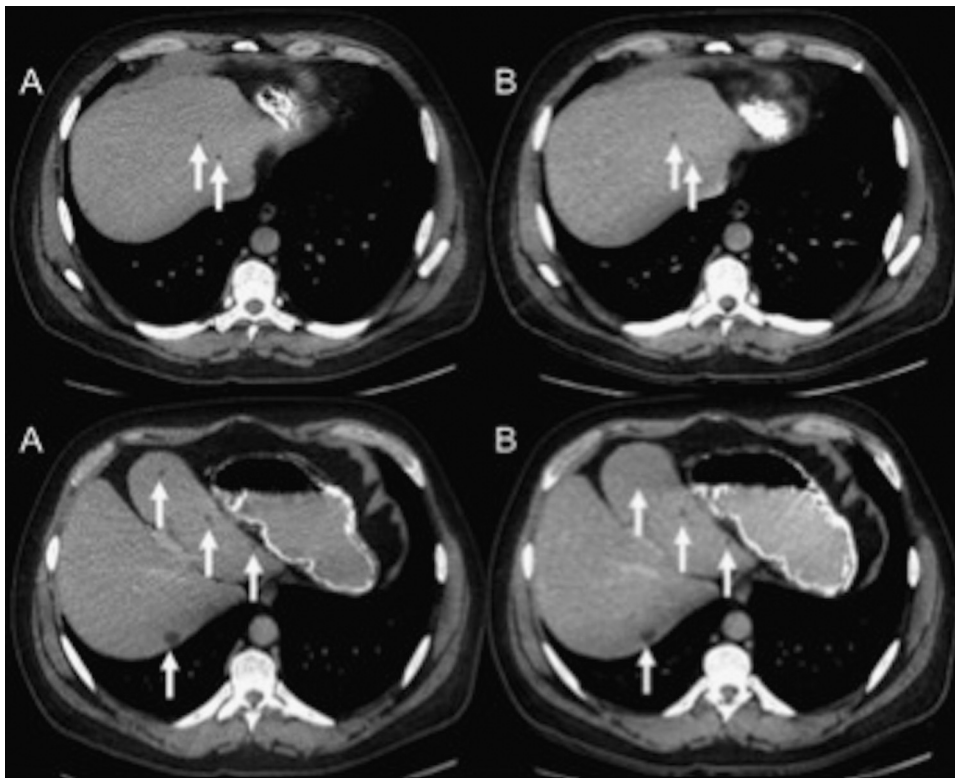


Fig. 7. Axial CT images from a 46-year-old study participant (BMI 31.3 kg/m²) that had a low-dose abdominopelvic CT performed for an ED of 2.64 mSv (B). Small hepatic cysts are visible on both CD–ASiR (A) and LD–MBiR (B) images.

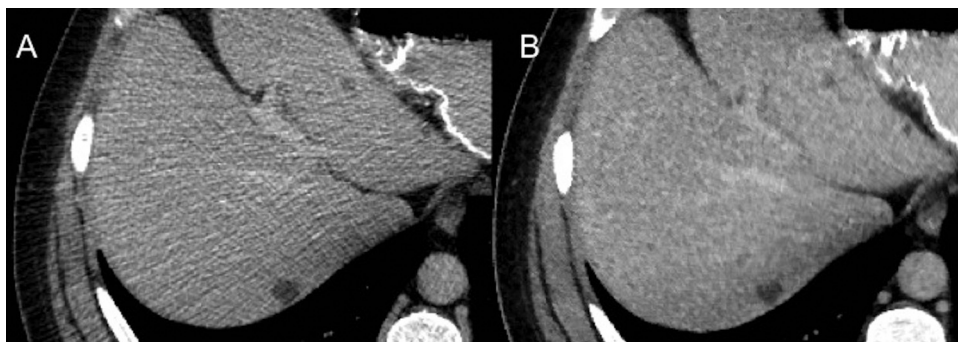


Fig. 8. Zoomed up axial CT images from the patient in Fig. 7 shows CD-ASiR (A) and LD-MBIR (B) images of the liver cysts.

MRI is being investigated as an alternative to CT in follow-up of these patients but CT remains the gold-standard method. MRI, when read by experienced radiologists, reportedly yields comparable results to CT in assessing the retroperitoneum in patients with testicular GCT [30]. A large on-going trial is investigating the use of MRI in stage I seminoma [TRISST Trial, Medical Research Council, UK; ClinicalTrials.gov identifier NCT00589537].

Reduced dose CT is a desirable alternative to conventional dose CT. Multiple strategies are available to reduce CT radiation dose – these include technical factors at the time of the study [28] in addition to alterations in frequency of surveillance [31]. Our results suggest that pure iterative reconstruction is a valuable additional technical CT dose reduction strategy.

A number of study limitations can be identified. It was considered unethical to subject patients to two studies that would have resulted in their receiving a total overall radiation dose in excess of our usual departmental protocol. Therefore, the total dose used in both CD and LD protocols was set at that which would have been received under normal protocols, with CD protocol utilised for this study conferring 70–80% of standard departmental protocol dose. Thus, CD images used for LD image comparison do not represent what would have been produced during conventional departmental scanning, but rather are derived from a dose slightly lower than usual. Nonetheless, it seems valid to use this slightly reduced dose dataset as a conventional dose benchmark, given that the study purpose was to confirm no loss of diagnostic capability with further, greater, dose reduction. Secondly, the radiation dose from the scanned projection radiograph (topogram) was excluded from dose calculation, per EU rules for assessing CT radiation dose, hence the dose per study was slightly underestimated. Thirdly, reviewer blinding as to the scanning protocol during clinical interpretation was not fully possible as LD-MBIR images had an obviously different appearance to CD-ASiR images. To reduce recall bias, randomised LD-MBIR datasets were read six weeks prior to randomised CD-ASiR dataset assessment. Iterative reconstruction algorithms from only a single vendor (GE Healthcare) were assessed. It must also be stated that a significant drawback of MBIR is the relatively long reconstruction time required (20–45 min per dataset at present) compared with near instantaneous hybrid IR. In the setting of outpatient CT scanning for testicular cancer surveillance, however, immediate image reconstruction is not required. Finally, these results are only directly applicable to follow-up of patients with testicular cancer though it is not unreasonable to surmise that it is an acceptable strategy for other patient cohorts.

In conclusion, our results show that reduced dose CT imaging, with pure model-based iterative reconstruction, may be an important tool in the future surveillance of testicular cancer patients.

References

- [1] UNSCEAR, Sources and Effects of Ionizing Radiation (2008).
- [2] D.J. Brenner, E.J. Hall, Computed tomography—an increasing source of radiation exposure, *N. Engl. J. Med.* 357 (2007) 2277–2284, <http://dx.doi.org/10.1056/NEJMra072149>.
- [3] A. Znaor, J. Lortet-Tieulent, A. Jemal, F. Bray, International variations and trends in testicular cancer incidence and mortality, *Eur. Urol.* 65 (2014) 1095–1096, <http://dx.doi.org/10.1016/j.eururo.2013.11.004>.
- [4] NCCN, Clinical Practice Guidelines in Oncology Version 1.2015 – Testicular Cancer, (2015).
- [5] J. Oldenburg, S.D. Fossà, J. Nuver, A. Heidenreich, H.-J. Schmolli, C. Bokemeyer, et al., Testicular seminoma and non-seminoma: ESMO clinical practice guidelines for diagnosis, treatment and follow-up, *Ann Oncol.* 24 (Suppl 6) (2013) 25–32, <http://dx.doi.org/10.1093/annonc/mdt304>, vi1.
- [6] R.A. Huddart, A. Norman, M. Shahidi, A. Horwich, D. Coward, J. Nicholls, et al., Cardiovascular disease as a long-term complication of treatment for testicular cancer, *J. Clin. Oncol.* 21 (2003) 1513–1523, <http://dx.doi.org/10.1200/JCO.2003.04.173>.
- [7] G.K. Zagars, M.T. Ballo, A.K. Lee, S.S. Strom, Mortality after cure of testicular seminoma, *J. Clin. Oncol.* 22 (2004) 640–647, <http://dx.doi.org/10.1200/JCO.2004.05.205>.
- [8] C.J. Beard, L.B. Travis, M.-H. Chen, N.D. Arvold, P.L. Nguyen, N.E. Martin, et al., Outcomes in stage I testicular seminoma: a population-based study of 9193 patients, *Cancer* 119 (2013) 2771–2777, <http://dx.doi.org/10.1002/ncr.28086>.
- [9] L.B. Travis, S.D. Fossà, S.J. Schonfeld, M.L. McMaster, C.F. Lynch, H. Storm, et al., Second cancers among 40,576 testicular cancer patients: focus on long-term survivors, *J. Natl. Cancer Inst.* 97 (2005) 1354–1365, <http://dx.doi.org/10.1093/jnci/dji278>.
- [10] C.J. Sullivan, K.P. Murphy, P.D. McLaughlin, M. Twomey, K.N. O'Regan, D.G. Power, et al., Radiation exposure from diagnostic imaging in young patients with testicular cancer, *Eur. Radiol.* 25 (2014) 1005–1013, <http://dx.doi.org/10.1007/s00330-014-3507-0>.
- [11] M.V. Silva, P. Motamedinia, G.M. Badalato, G. Hruby, J.M. McKiernan, Diagnostic radiation exposure risk in a contemporary cohort of male patients with germ cell tumor, *J. Urol.* 187 (2012) 482–486, <http://dx.doi.org/10.1016/j.juro.2011.10.028>.
- [12] O.J. O'Connell, S. McWilliams, A. McGarrigle, O.J. O'Connor, F. Shanahan, D. Mullane, et al., Radiologic imaging in cystic fibrosis: cumulative effective dose and changing trends over 2 decades, *Chest* 141 (2012) 1575–1583, <http://dx.doi.org/10.1378/chest.11-1972>.
- [13] S.M. Kinsella, J.P. Coyle, E.B. Long, S.R. McWilliams, M.M. Maher, M.R. Clarkson, et al., Maintenance hemodialysis patients have high cumulative radiation exposure, *Kidney Int.* 78 (2010) 789–793, <http://dx.doi.org/10.1038/ki.2010.196>.
- [14] J. Coyle, S. Kinsella, S. McCarthy, S. MacWilliams, P. McLaughlin, J. Eustace, et al., Cumulative ionizing radiation exposure in patients with end stage kidney disease: a 6-year retrospective analysis, *Abdom. Imaging* 37 (2012) 632–638, <http://dx.doi.org/10.1007/s00261-011-9786-x>.
- [15] A.N. Desmond, S. McWilliams, M.M. Maher, F. Shanahan, E.M. Quigley, Radiation exposure from diagnostic imaging among patients with gastrointestinal disorders, *Clin. Gastroenterol. Hepatol.* 10 (2012) 259–265, <http://dx.doi.org/10.1016/j.cgh.2011.11.007>.
- [16] O. Craig, S. O'Neill, F. O'Neill, P. McLaughlin, A. McGarrigle, S. McWilliams, et al., Diagnostic accuracy of computed tomography using lower doses of radiation for patients with Crohn's disease, *Clin. Gastroenterol. Hepatol.* 10 (2012) 886–892, <http://dx.doi.org/10.1016/j.cgh.2012.03.014>.
- [17] S. Singh, M.K. Kalra, J. Hsieh, P.E. Licato, S. Do, H.H. Pien, et al., Abdominal CT: comparison of adaptive statistical iterative and filtered back projection reconstruction techniques, *Radiology* 257 (2010) 373–383, <http://dx.doi.org/10.1148/radiol.10092212>.
- [18] S. Singh, M.K. Kalra, S. Do, J.B. Thibault, H. Pien, O.J. O'Connor, et al., Comparison of hybrid and pure iterative reconstruction techniques with conventional filtered back projection: dose reduction potential in the

- abdomen, *J. Comput. Assisted Tomogr.* 36 (2012) 347–353, <http://dx.doi.org/10.1097/RCT.0b013e31824e639e>.
- [19] Z. Deák, J.M. Grimm, M. Treitl, L.L. Geyer, U. Linsenmaier, M. Körner, et al., Filtered back projection, adaptive statistical iterative reconstruction, and a model-based iterative reconstruction in abdominal CT: an experimental clinical study, *Radiology* 266 (2013) 197–206, <http://dx.doi.org/10.1148/radiol.12112707>.
- [20] M. Katsura, I. Matsuda, M. Akahane, J. Sato, H. Akai, K. Yasaka, et al., Model-based iterative reconstruction technique for radiation dose reduction in chest CT: comparison with the adaptive statistical iterative reconstruction technique, *Eur. Radiol.* 22 (2012) 1613–1623, <http://dx.doi.org/10.1007/s00330-012-2452-z>.
- [21] K. Yasaka, M. Katsura, M. Akahane, J. Sato, I. Matsuda, K. Ohtomo, Model-based iterative reconstruction for reduction of radiation dose in abdominopelvic CT: comparison to adaptive statistical iterative reconstruction, *Springerplus* 2 (2013) 209, <http://dx.doi.org/10.1186/2193-1801-2-209>.
- [22] W.P. Shuman, K.T. Chan, J.M. Busey, L.M. Mitsumori, E. Choi, K.M. Koprowicz, et al., Standard and reduced radiation dose liver ct images: adaptive statistical iterative reconstruction versus model-based iterative reconstruction-comparison of findings and image quality, *Radiology* 273 (2014) 793–800, <http://dx.doi.org/10.1148/radiol.14140676>.
- [23] The 2007 Recommendations of the International Commission on Radiological Protection ICRP publication 103., *Ann. ICRP*, 37 (2007). 1–332. 10.1016/j.icrp.2007.10.003.
- [24] J. Boone, K. Strauss, C. D. E. Al., Size-specific dose estimate (SSDE) in pediatric and adult body CT examinations Report of AAPM Task Group 204. College Park: American Association of Physicists in Medicine, (2011).
- [25] S.L. Brady, R.A. Kaufman, Investigation of American Association of Physicists in Medicine Report 204 size-specific dose estimates for pediatric CT implementation, *Radiology* 265 (2012) 832–840, <http://dx.doi.org/10.1148/radiol.12120131>.
- [26] V.P. Jackson, T. Cushing, H.H. Abujudeh, J.P. Borgstede, K.W. Chin, C.K. Grimes, et al., RADPEER scoring white paper, *J. Am. Coll. Radiol.* 6 (2009) 21–25, <http://dx.doi.org/10.1016/j.jacr.2008.06.011>.
- [27] M.E. O'Malley, P. Chung, M. Haider, H.-J. Jang, K. Jhaveri, K. Khalili, et al., Comparison of low dose with standard dose abdominal/pelvic multidetector CT in patients with stage 1 testicular cancer under surveillance, *Eur. Radiol.* 20 (2010) 1624–1630, <http://dx.doi.org/10.1007/s00330-009-1710-1>.
- [28] R. Gnannt, A. Winklehner, D. Eberli, A. Knuth, T. Frauenfelder, H. Alkadhi, Automated tube potential selection for standard chest and abdominal CT in follow-up patients with testicular cancer: comparison with fixed tube potential, *Eur. Radiol.* 22 (2012) 1937–1945, <http://dx.doi.org/10.1007/s00330-012-2453-y>.
- [29] M. Meyer, S.A. Klein, G. Brix, C. Fink, L. Pilz, H. Jafarov, et al., Whole-body CT for lymphoma staging: feasibility of halving radiation dose and risk by iterative image reconstruction, *Eur. J. Radiol.* 83 (2014) 315–321, <http://dx.doi.org/10.1016/j.ejrad.2013.11.008>.
- [30] H.K. Kok, S. Leong, W.C. Torreggiani, Is magnetic resonance imaging comparable with computed tomography in the diagnosis of retroperitoneal metastasis in patients with testicular cancer? *Can. Assoc. Radiol. J.* 65 (2014) 196–198, <http://dx.doi.org/10.1016/j.carj.2013.05.005>.
- [31] G.J. Rustin, G.M. Mead, S.P. Stenning, P.A. Vasey, N. Aass, R.A. Huddart, et al., Randomized trial of two or five computed tomography scans in the surveillance of patients with stage I nonseminomatous germ cell tumors of the testis: Medical Research Council Trial TE08, ISRCTN56475197—the National Cancer Research Institute Testis Cancer Clinical Studies Group, *J. Clin. Oncol.* 25 (2007) 1310–1315, <http://dx.doi.org/10.1200/JCO.2006.08.4889>.